Nuclear structure of ^{74}Ge from inelastic neutron scattering measurements and shell-model calculations

E. E. Peters,[1,*] B. A. Brown,[2,3] S. Mukhopadhyay,[1,4,†] A. P. D. Ramirez,[1,4,‡] and S. W. Yates[1,4,§]

[1]*Department of Chemistry, University of Kentucky, Lexington, Kentucky 40506-0055, USA*
[2]*The Facility for Rare Isotope Beams, Michigan State University, East Lansing, Michigan 48824, USA*
[3]*Department of Physics and Astronomy, Michigan State University, East Lansing, Michigan 48824, USA*
[4]*Department of Physics and Astronomy, University of Kentucky, Lexington, Kentucky 40506-0055, USA*

(Received 4 August 2023; accepted 20 March 2024; published 20 May 2024)

The low-lying, low-spin levels of ^{74}Ge were studied with the $(n, n'\gamma)$ reaction. γ-ray excitation function measurements were performed at incident neutron energies from 1.6 to 3.8 MeV, and γ-ray angular distributions were measured at neutron energies of 2.0, 2.6, 3.0, 3.4, and 3.8 MeV. From these measurements, level spins, level lifetimes, γ-ray branching ratios, and multipole mixing ratios were determined, and a comprehensive level scheme approaching 3 MeV in excitation energy is presented. Low-lying collective band structures are identified, and a comparison of the level characteristics with large-scale shell-model calculations yields excellent agreement.

DOI: 10.1103/PhysRevC.109.054318

I. INTRODUCTION

The stable germanium nuclei exhibit a number of interesting structural features including shape coexistence [1,2] and triaxiality [3–6], but recent interest in these nuclei has been motivated by the emergence of ^{76}Ge as one of the best candidates for the observation of neutrinoless double-β ($0\nu\beta\beta$) decay [7].

If observed, $0\nu\beta\beta$ decay provides perhaps the best method for obtaining the mass of the electron neutrino, and it is the only practical way to establish if neutrinos are Majorana particles. The rate of $0\nu\beta\beta$ is approximately the product of (a) the known phase-space factor for the emission of two electrons, (b) the effective Majorana mass of the electron neutrino, and (c) the nuclear matrix element (NME) for the ^{76}Ge to ^{76}Se transition. The NME cannot be determined experimentally and, therefore, must be calculated from nuclear structure models. In recent studies of ^{76}Ge [8] and ^{76}Se [9] with the $(n, n'\gamma)$ reaction, we have focused on providing detailed nuclear structure information to constrain these calculations; however, additional data from other nuclei in the vicinity can be utilized to refine these model calculations further [10]. To better characterize this transitional region, studies of other stable Ge nuclei have been initiated; the study of ^{74}Ge reported here is the first of these additional inquiries.

Recent investigations of the low-lying, low-spin levels of ^{74}Ge are rare; most notable among these, however, are the work by Sun *et al.* [11] with the ^{70}Zn(^{7}Li, $p2n\gamma$) reaction and the $(n, n'\gamma)$ reaction study by Kosyak, Chekushina, and Ermatov [12] with reactor fast neutrons. Photon scattering measurements [13,14] and $(\alpha, \alpha'\gamma)$ reaction data [15] have contributed new information about spin-1 states. Unpublished data from a ^{73}Ge(n, γ) study at the Institut Laue Langevin-Grenoble [16] proved useful for comparing with the data from our measurements, and data from recent two-neutron transfer and deep inelastic scattering measurements, i.e., the ^{76}Ge + ^{238}U and ^{70}Zn + ^{208}Pb reactions leading to ^{74}Ge as one of the final nuclei, were available to us [17]. In addition, a state-of-the-art nuclear resonance fluorescence study with quasi-monoenergetic, linearly polarized photon beams has recently been performed at the High-Intensity Gamma-Ray Source (HIγS) at Triangle Universities Nuclear Laboratory (TUNL) as part of a collaborative effort for our studies of the Ge isotopes [18].

The $(n, n'\gamma)$ reaction exhibits several advantages over other in-beam reactions. With no Coulomb barrier, nearly monoenergetic accelerator-produced neutrons can excite the nucleus to any degree desirable. The reaction is also nonselective allowing the population of nonyrast states. Detection of the emitted γ rays provides good energy resolution, and level lifetimes can be determined with Doppler-shift attenuation methods [19]. A disadvantage of the technique is that large amounts (i.e., several grams in most cases) of enriched isotopes are often required to obtain reasonable counting rates. In addition, although the cross sections for inelastic scattering are typically not small, the neutron fluences for these secondary reactions are limited. However, from these measurements, levels are identified, and the cross sections obtained from the excitation functions provide information about

*fe.peters@uky.edu
†Present address: Nuclear and Radiological Engineering and Medical Physics Program, Georgia Institute of Technology, Atlanta, Georgia 30332, USA.
‡Present address: Nuclear and Chemical Sciences Division, Lawrence Livermore National Laboratory, Livermore, California 94550, USA.
§yates@uky.edu

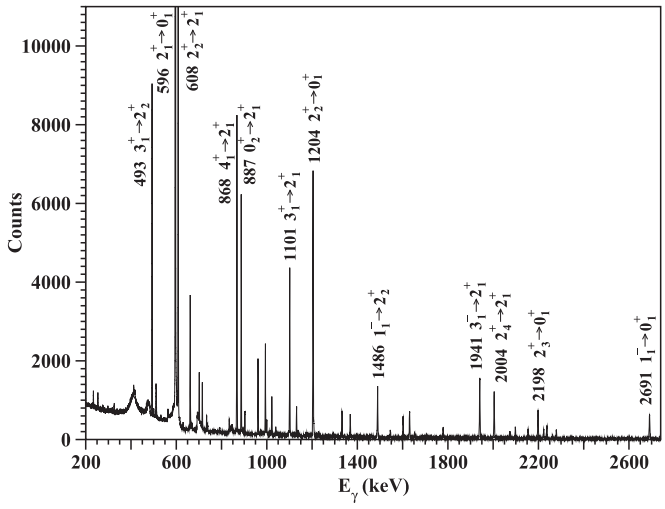

FIG. 1. γ-ray spectrum from 3.0 MeV neutrons incident on the enriched ^{74}Ge scattering sample at a detection angle of 90°. The most intense γ rays are labeled with their energies and the transitions they represent.

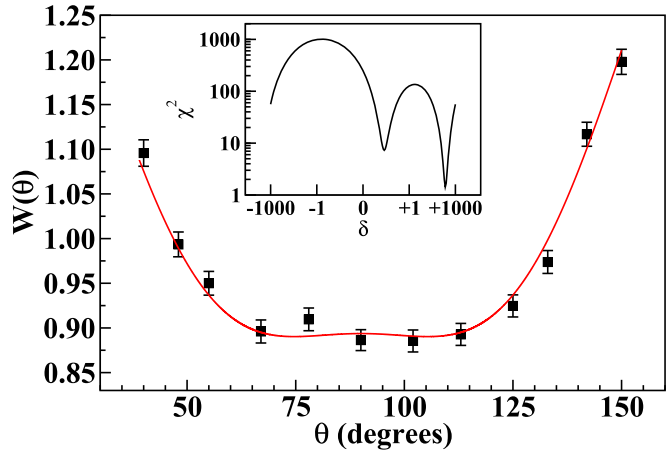

FIG. 2. Angular distribution of the 1101.3 keV γ ray from the 1697.3 keV 3^+ state to the 595.9 keV 2^+ state. The $E2/M1$ mixing ratio, δ, determined from these data is $+5.84^{+48}_{-60}$.

the spins and parities of the populated levels. Furthermore, from level lifetimes, γ-ray branching ratios, and multipole mixing ratios, reduced transition probabilities can be obtained. Thus, a wealth of information can be gained from this single reaction.

While it is also clear that some properties, e.g., magnetic dipole and electric quadrupole moments, cannot be determined in our work, the quantities available from our data, allow the development of a comprehensive level scheme and provide detailed quantities for comparison with theoretical calculations.

II. EXPERIMENTAL DETAILS AND DATA ANALYSIS

Using the methods described in detail for ^{76}Ge and ^{76}Se [8,9], we performed ^{74}Ge$(n, n'\gamma)$ measurements at the University of Kentucky Accelerator Laboratory (UKAL). The ^{3}H$(p, n)^3$He reaction with a tritium gas target and a time-bunched proton beam produced fast neutrons which impinged on a scattering sample consisting of 19.3406 g of elemental Ge powder enriched to 98.9% in ^{74}Ge in a cylindrical polyethylene vial of 1.14 cm radius and 3.58 cm height. γ rays were detected with a high-purity germanium (HPGe) detector of ≈50% relative efficiency and energy resolution of 2.0 keV (full width at half-maximum) at 1333 keV surrounded by a bismuth germanate (BGO) annulus, which functioned as a Compton suppressor and active shield. ^{24}Na and ^{137}Cs radioactive sources were placed near the detector to provide online calibrations. ^{56}Co and ^{226}Ra were used offline for efficiency and nonlinearity calibrations. A portion of the in-beam γ-ray spectrum is shown in Fig. 1.

For the excitation function measurements, γ-ray spectra were recorded at incident neutron energies from 1.6 to 3.8 MeV in 0.10 MeV steps and an angle of 125° relative to the beam axis. γ rays were placed in the level scheme from their energy thresholds. Relative experimental level cross sections were compared with cross sections computed with the statistical model code CINDY [20] to infer spins of the levels.

At incident neutron energies of 2.0, 2.6, 3.0, 3.4, and 3.8 MeV, γ-ray spectra were measured at eleven angles from 40° to 150° relative to the beam axis. The yield of a γ ray can be fit with a least-squares Legendre polynomial expansion in which only the even-order terms contribute and the angular distribution coefficients a_2 and a_4 depend on the level spins, transition multipolarities, and multipole mixing ratios. Figure 2 illustrates the angular distribution of the 1101.3 keV γ ray from the 1697.3 keV 3^+ level to the first excited state of ^{74}Ge and the $E2/M1$ mixing ratio, δ, that was determined by comparison with CINDY [20] calculations. The adopted J value is that for which the χ^2 value is at a minimum; when similar minima result for more than one spin value, the one for which all branches agree is chosen, or multiple spins possibilities are listed. The excitation function data are also of value as mentioned above. The adopted mixing ratio is that for which the χ^2 value is at a minimum for the determined spin. If two minima are present with a small difference in χ^2, both δ values are reported. It is worth noting that transitions with measurable $M2$ components are not observed in our experiments, thus those transitions involving changes in parity are taken to be pure $E1$ transitions by this population mechanism. Ground-state transitions are either pure $E2$, $E1$, or $M1$ as determined by the changes in multipolarity and angular momentum, which are based upon the sign of the a_2 coefficient and the measured multipole mixing ratio. Pure multipolarity for any transition is determined when the minimum χ^2 value corresponds to a δ of 0 within uncertainties.

These spectra can also be used to determine level lifetimes with the Doppler-shift attenuation method. An example is given in Fig. 3, where the lifetime of the 2833.0 keV 2^+ state is determined from the Doppler shift of the 2237.1 keV γ ray.

III. EXPERIMENTAL RESULTS

Results from the $(n, n'\gamma)$ measurements performed at UKAL are summarized in Table I in which only data from

TABLE I. Data extracted exclusively from the present $(n, n'\gamma)$ experiments for ^{74}Ge. New levels and γ rays are in **bold**. Multipole mixing ratios are reported using the Krane and Steffen sign convention [21]. When two mixing ratios are possible, the solution with the lowest χ^2 value is listed first.

E_{initial} (keV)	E_γ (keV)	E_{final} (keV)	J_i^π	J_f^π	B.R.	$\bar{F}(\tau)$	τ_{level} (fs)	δ or multipolarity	$B(E2)$ (W.u.)	$B(M1)$ (μ_N^2)	$B(E1)$ (mW.u.)
595.886(9)	595.882(10)	0.0	2^+	0^+	1.000			$E2$			
1204.293(11)	608.389(10)	595.9	2^+	2^+	0.670(3)			$+2.98^{+10}_{-20}$			
	1204.266(25)	0.0		0^+	0.330(3)			$E2$			
1463.882(14)	867.961(21)	595.9	4^+	2^+	1.000	0.023(7)	2350^{+990}_{-540}	$E2$	38(11)		
1482.902(15)	886.986(23)	595.9	0^+	2^+	1.000	0.017(6)	3700^{+2200}_{-1100}	$E2$	21.9(83)		
1697.267(12)	233.368(25)	1463.9	3^+	4^+	0.010(1)	0.002(7)	> 4530	$+0.9^{+14}_{-3}$	< 66	<0.0053	
	492.974(10)	1204.3		2^+	0.484(6)			$+2.07^{+15}_{-10}$	< 130	<0.0096	
	1101.319(20)	595.9		2^+	0.506(6)			$+5.84^{+48}_{-60}$	<3.0	<0.00014	
2165.449(15)	468.158(26)	1697.3	4^+	3^+	0.026(2)	0.035(14)	1600^{+1100}_{-500}	$+1.06^{+91}_{-42}$	17^{+22}_{-12}	0.0043^{+56}_{-33}	
	701.551(10)	1463.9		4^+	0.318(5)			$+0.84^{+10}_{-11}$	22^{+14}_{-11}	0.020^{+12}_{-9}	
								0.138^{+69}_{-59}	1.0^{+21}_{-8}	0.033^{+15}_{-14}	
	961.183(24)	1204.3		2^+	0.656(5)			$E2$	22.4(94)		
2198.084(12)	715.160(10)	1482.9	2^+	0^+	0.135(2)	0.034(5)	1610^{+270}_{-200}	$E2$	19.8^{+32}_{-31}		
	734.194(20)	1463.9		4^+	0.040(1)			$E2$	5.15^{+88}_{-85}		
	993.759(24)	1204.3		2^+	0.383(5)			$+0.99^{+11}_{-13}$	5.4(15)	0.0070^{+23}_{-17}	
								$+0.422^{+88}_{-62}$	1.64^{+95}_{-59}	0.0117^{+24}_{-25}	
	1602.136(17)	595.9		2^+	0.128(2)			$+4.87^{+86}_{-70}$	0.320^{+55}_{-54}	0.000044^{+25}_{-17}	
								-0.201^{+26}_{-23}	0.0129^{+55}_{-46}	0.00106^{+18}_{-17}	
	2198.058(20)	0.0		0^+	0.313(6)			$E2$	0.168(27)		
2226.548(19)	1022.244(21)	1204.3	0^+	2^+	0.474(5)	0.010(7)	> 3270	$E2$	<5.7		
	1630.613(22)	595.9		2^+	0.526(5)			$E2$	<0.62		
2536.576(14)	839.297(84)	1697.3	3^-	3^+	0.018(1)	0.151(11)	341^{+32}_{-28}	$E1$			0.0494^{+74}_{-68}
	1332.251(12)	1204.3		2^+	0.204(5)			$E1$			0.140^{+16}_{-15}
	1940.692(30)	595.9		2^+	0.778(5)			$E1$			0.173^{+17}_{-16}
2569.34(22)	1105.43(19)	1463.9	6^+	4^+	1.000	0.079(39)	750^{+810}_{-270}	$E2$	36^{+20}_{-18}		
2600.329(15)	**903.077(16)**	1697.3	2^+	3^+	0.099(4)	0.076(8)	721^{+81}_{-72}	$+1.54^{+87}_{-91}$	7.1^{+29}_{-46}	0.0031^{+56}_{-18}	
	1395.969(52)	1204.3		2^+	0.022(1)			-4.6^{+20}_{-44}	0.243^{+49}_{-52}	0.000029^{+64}_{-22}	
								-0.70^{+16}_{-23}	0.084^{+54}_{-34}	0.00043(14)	
	2004.355(16)	595.9		2^+	0.847(9)			-0.002^{+18}_{-14}	0.000006^{+460}_{-6}	0.0083^{+10}_{-9}	
	2600.348(87)	0.0		0^+	0.032(9)			$E2$	0.0165^{+70}_{-58}		
2669.701(22)	972.402(28)	1697.3	4^+	3^+	0.154(4)	0.050(12)	1200^{+410}_{-250}	$+0.76^{+18}_{-12}$	2.4^{+16}_{-10}	0.0051^{+23}_{-20}	
								$+1.50^{+39}_{-93}$	4.5^{+21}_{-34}	0.0024^{+53}_{-12}	
	2073.766(22)	595.9		2^+	0.846(4)			$E2$	0.81^{+22}_{-21}		
2690.720(36)	**1486.437(54)**	1204.3	1	2^+	0.095(6)	0.164(10)	303^{+24}_{-21}				
	2690.639(40)	0.0		0^+	0.905(6)						
2693.827(15)	1489.479(11)	1204.3	3^-	2^+	0.719(7)	0.030(9)	2020^{+840}_{-460}	$E1$			0.060(18)
	2097.938(21)	595.9		2^+	0.281(7)			$E1$			0.0083^{+27}_{-26}
2697.139(18)	531.625(44)	2165.4	5^+	4^+	0.113(5)	0.069(13)	790^{+200}_{-130}	$+0.51^{+15}_{-11}$	30^{+26}_{-15}	0.043^{+16}_{-14}	
	999.845(13)	1697.3		3^+	0.887(5)			$E2$	50(10)		
2750.124(35)	1545.796(32)	1204.3	0^+	2^+	0.332(9)	0.048(14)	1160^{+480}_{-270}	$E2$	1.43^{+49}_{-45}		
	2154.129(81)	595.9		2^+	0.668(9)			$E2$	0.55^{+18}_{-17}		
2828.747(16)	1131.443(10)	1697.3	4^-	3^+	1.000	0.022(10)	2800^{+2600}_{-1000}	$E1$			0.137^{+67}_{-66}
2833.045(59)	**1628.5(4)**	1204.3	2^+	2^+	0.031(8)	0.694(11)	28(1)	$E2/M1$	$\leqslant 4.3$	$\leqslant 0.015$	
	2237.108(53)	595.9		2^+	0.969(8)			$+0.014^{+33}_{-30}$	0.005^{+58}_{-5}	0.176(8)	

TABLE I. (*Continued.*)

E_{initial} (keV)	E_γ (keV)	E_{final} (keV)	J_i^π	J_f^π	B.R.	$\bar{F}(\tau)$	τ_{level} (fs)	δ or multipolarity	$B(E2)$ (W.u.)	$B(M1)$ (μ_N^2)	$B(E1)$ (mW.u.)
								$+2.31^{+22}_{-19}$	23.0^{+17}_{-16}	0.0277^{+56}_{-49}	
2836.280(22)	670.8[a]	2165.4	4^+	4^+	0.128(32)	0.124(17)	448^{+82}_{-63}	$E2/M1$	$\leqslant 93$	$\leqslant 0.054$	
	1138.974(18)	1697.3		3^+	0.232(35)			$+5.11^{+62}_{-64}$	11.5^{+40}_{-33}	0.00074^{+54}_{-31}	
	1372.342(58)	1463.9		4^+	0.059(9)			-1.3^{+3}_{-11}	0.76^{+61}_{-34}	0.00107^{+94}_{-76}	
	1632.006(86)	1204.3		2^+	0.49(12)			$E2$	4.2^{+19}_{-15}		
	2240.4(9)	595.9		2^+	0.092(23)			$E2$	0.161^{+73}_{-59}		
2857.297(24)	1652.952(20)	1204.3	0^+	2^+	0.547(7)	0.179(12)	291^{+24}_{-22}	$E2$	6.74^{+64}_{-59}		
	2261.389(64)	595.9		2^+	0.453(7)			$E2$	1.16^{+12}_{-11}		
2874.978(20)	**1177.633(25)**	1697.3	(3^+)	3^+	0.108(2)	0.182(10)	284^{+20}_{-18}	-0.517^{+65}_{-74}	1.57^{+52}_{-41}	0.0104^{+15}_{-14}	
	2279.062(21)	595.9		2^+	0.892(2)			$+0.342^{+18}_{-17}$	0.237^{+41}_{-35}	0.0135(11)	
2925.666(26)	1228.399(29)	1697.3	4^+	3^+	0.645(5)	0.087(9)	652^{+88}_{-68}	$+0.355^{+23}_{-30}$	1.75^{+45}_{-44}	0.0270^{+39}_{-37}	
	1461.630(45)	1463.9		4^+	0.083(2)			-2.5^{+11}_{-38}	0.73^{+21}_{-24}	0.00032^{+56}_{-27}	
	1721.361(99)	1204.3		2^+	0.147(3)			$E2$	0.660^{+92}_{-90}		
	2329.720(45)	595.9		2^+	0.125(4)			$E2$	0.124^{+19}_{-18}		
2935.768(46)	1471.839(39)	1463.9	5^-	4^+	1.000	0.032(19)	2000^{+3100}_{-800}	$E1$			0.086^{+54}_{-52}
2938.802(25)	**1734.390(59)**	1204.3	$2, 3^+$	2^+	0.105(3)	0.360(11)	115(5)				
	2342.865(22)	595.9		2^+	0.895(3)						
2949.481(23)	1745.047(39)	1204.3	(2^-)	2^+	0.083(3)	0.066(10)	880^{+170}_{-130}	$(E1)$			0.0099^{+21}_{-19}
	2353.562(22)	595.9		2^+	0.917(3)			$(E1)$			0.0444^{+77}_{-73}
2973.709(54)	808.268(58)	2165.4	5^-	4^+	0.325(12)			$E1$			
	1509.710(77)	1463.9		4^+	0.675(12)			$E1$			
2999.198(23)	**1301.903(46)**	1697.3	2^+	3^+	0.049(2)	0.405(11)	95(4)	$+0.13^{+11}_{-10}$	0.11^{+26}_{-10}	0.0131^{+14}_{-15}	
	1794.69(44)	1204.3		2^+	0.042(3)			-0.29^{+21}_{-26}	0.08^{+19}_{-8}	0.0040^{+8}_{-10}	
	2403.247(24)	595.9		2^+	0.739(7)			-0.262^{+22}_{-29}	0.276^{+77}_{-54}	0.0298(19)	
								$+6.9^{+22}_{-11}$	4.20^{+27}_{-24}	0.00066^{+33}_{-30}	
	2999.125(45)	0.0		0^+	0.170(6)			$E2$	0.326^{+26}_{-24}		
3017.783(22)	**1320.340(84)**	1697.3	(2^+)	3^+	0.021(1)	0.697(9)	30(1)	$+0.08(21)$	0.05^{+60}_{-5}	0.0172^{+16}_{-25}	
	1813.390(26)	1204.3		2^+	0.442(5)			$+0.019^{+28}_{-35}$	0.012^{+65}_{-12}	0.140^{+7}_{-6}	
								$+2.25^{+27}_{-21}$	27.8^{+23}_{-21}	0.0231^{+53}_{-49}	
	2421.894(27)	595.9		2^+	0.537(5)			$+4.7^{+10}_{-5}$	9.08^{+54}_{-47}	0.0031^{+10}_{-11}	
								$-0.191(33)$	0.33^{+14}_{-11}	0.0691^{+39}_{-37}	
3032.888(34)	3032.821(30)	0.0	1	0^+	1.000	0.562(14)	52(3)				
3034.147(19)[b]	497.540(17)	2536.6	3^+	3^-	0.158-0.290	0.042(16)	1400^{+860}_{-400}	$E1$			0.51-0.93
	1336.828(38)	1697.3		3^+	0.187-0.343			-0.022^{+53}_{-57}	0.00067-0.0012	0.0032-0.0058	
								$+1.53^{+23}_{-20}$	0.97-1.8	0.00096-0.0018	
	1570.234(25)	1463.9		4^+	0.155-0.284			$+0.028^{+51}_{-59}$	0.00040-0.00074	0.0016-0.0030	
								-10^{+3}_{-11}	0.51-0.93	0.000017-0.000031	
	1829.9[a]	1204.3		2^+	$\leqslant 0.455$				$\leqslant 0.70$	$\leqslant 0.0030$	
	2438.43(18)	595.9		2^+	0.045-0.083			-2.8^{+7}_{-11}	0.015-0.027	0.000015-0.000027	
								-0.16^{+10}_{-11}	0.00044-0.00081	0.00012-0.00023	
3048.769(25)	850.582(55)	2198.1	4^+	2^+	0.102(4)	0.078(28)	730^{+430}_{-210}	$E2$	14.0^{+63}_{-56}		

TABLE I. (*Continued.*)

E_{initial} (keV)	E_γ (keV)	E_{final} (keV)	J_i^π	J_f^π	B.R.	$\bar{F}(\tau)$	τ_{level} (fs)	δ or multipolarity	$B(E2)$ (W.u.)	$B(M1)$ (μ_N^2)	$B(E1)$ (mW.u.)
	883.301(21)	2165.4		4^+	0.403(7)			-0.114^{+67}_{-61}	0.6^{+13}_{-5}	0.045^{+20}_{-18}	
	1844.27(10)	1204.3		2^+	0.384(6)			$E2$	1.10^{+46}_{-42}		
	2452.848(78)	595.9		2^+	0.111(4)			$E2$	0.076^{+34}_{-30}		
3081.680(23)	545.075(39)	2536.6	4^-	3^-	0.137(5)	0.110(13)	493^{+78}_{-58}	-0.267^{+60}_{-75}	17^{+14}_{-8}	0.091^{+19}_{-18}	
	1384.376(24)	1697.3		3^+	0.289(5)			$E1$			0.122(19)
	1617.729(35)	1463.9		4^+	0.574(6)			$E1$			0.152(22)
3092.337(27)	1887.961(33)	1204.3	1^+	2^+	0.460(10)	0.685(12)	31(2)	-5^{+2}_{-11}	26.1^{+37}_{-44}	0.006^{+13}_{-5}	
								$+0.07^{+15}_{-17}$	0.1^{+13}_{-1}	0.125^{+12}_{-15}	
	2496.459(80)	595.9		2^+	0.075(4)			-0.7^{+8}_{-27}	0.39^{+75}_{-39}	0.0057^{+43}_{-51}	
	3092.281(37)	0.0		0^+	0.465(12)			$M1$		0.0288^{+28}_{-25}	
3104.827(54)	939.342(46)	2165.4	5^-	4^+	1.000	0.031(95)	> 423	$E1$			<1.6
3140.704(17)	604.170(30)	2536.6	3^-	3^-	0.177(9)	0.084(14)	660^{+150}_{-100}	-0.37^{+9}_{-11}	17^{+16}_{-9}	0.061^{+19}_{-17}	
								$+4.3^{+27}_{-13}$	140^{+40}_{-36}	0.0035^{+47}_{-24}	
	942.558(27)	2198.1		2^+	0.168(5)			$E1$			0.167^{+37}_{-34}
	975.54(15)	2165.4		4^+	0.051(4)			$E1$			0.046^{+13}_{-11}
	1443.375(16)	1697.3		3^+	0.488(8)			$E1$			0.135^{+28}_{-26}
	1676.67(10)	1463.9		4^+	0.115(4)			$E1$			0.0204^{+46}_{-42}
3175.538(17)	638.940(10)	2536.6	3^-	3^-	0.286(4)	0.176(11)	287^{+23}_{-21}	-0.335^{+27}_{-43}	42^{+15}_{-9}	0.195(22)	
	1478.279(75)	1697.3		3^+	0.092(3)			$E1$		0.0549^{+63}_{-57}	
	1971.112(29)	1204.3		2^+	0.179(4)			$E1$		0.0451^{+47}_{-43}	
	2579.696(62)	595.9		2^+	0.443(6)			$E1$		0.0498^{+47}_{-43}	
3180.078(66)	**1482.662(72)**	1697.3	$(2, 3, 4^+)$	3^+	0.723(13)	0.344(30)	129^{+18}_{-15}				
	2584.301(98)	595.9		2^+	0.277(13)						
3199.321(26)	**1501.981(40)**	1697.3	2^+	3^+	0.167(4)	0.217(10)	239^{+14}_{-13}	-0.6^{+2}_{-11}	1.0^{+23}_{-5}	0.0090^{+22}_{-62}	
	1994.964(33)	1204.3		2^+	0.479(6)			-0.011^{+42}_{-52}	0.0003^{+120}_{-3}	0.0144(10)	
								$+2.41^{+36}_{-29}$	2.39^{+27}_{-25}	0.00210^{+68}_{-57}	
	2603.61(11)	595.9		2^+	0.175(5)			-0.35^{+12}_{-14}	0.029^{+28}_{-17}	0.00210^{+34}_{-36}	
	3199.226(47)	0.0		0^+	0.179(6)			$E2$	0.0988^{+92}_{-86}		
3219.856(35)	**1054.405(43)**	2165.4	(5^+)	4^+	0.143(6)	0.278(15)	173^{+13}_{-12}	$+0.47^{+12}_{-9}$	5.0^{+31}_{-19}	0.0329(64)	
	1755.884(38)	1463.9		4^+	0.857(6)			$+0.337^{+41}_{-29}$	1.34^{+44}_{-29}	0.0467(47)	
3271.366(42)	1574.019(38)	1697.3	(4^-)	3^+	0.503(8)	0.100(20)	580^{+160}_{-110}	$(E1)$			0.123^{+30}_{-28}
	1807.65(12)	1463.9		4^+	0.497(8)			$(E1)$			0.080^{+19}_{-18}
3275.692(35)	**1077.463(52)**	2198.1	1	2^+	0.267(7)	0.283(17)	168^{+14}_{-13}				
	2679.90(10)	595.9		2^+	0.117(7)						
	3275.651(41)	0.0		0^+	0.616(9)						
3336.758(28)	**1171.257(27)**	2165.4	$4, 5^+, 6^+$	4^+	0.383(15)	0.292(21)	160^{+17}_{-14}				
	1872.818(35)	1463.9		4^+	0.617(15)						
3342.903(25)	2138.531(26)	1204.3	$2, 3^+$	2^+	0.560(8)	0.379(14)	110(6)				
	2746.954(36)	595.9		2^+	0.440(8)						
3359.177(46)	**2763.212(40)**	595.9		2^+	1.000	0.150(23)	364^{+75}_{-56}				
3381.625(34)	**1684.250(66)**	1697.3	(3^-)	3^+	0.108(5)	0.233(18)	214^{+23}_{-20}	$(E1)$			0.0585^{+90}_{-81}
	2785.670(32)	595.9		2^+	0.892(5)			$(E1)$			0.107^{+12}_{-11}
3386.494(35)	**2181.988(64)**	1204.3	$2, 3, 4^+$	2^+	0.271(7)	0.224(17)	225^{+22}_{-20}				
	2790.567(34)	595.9		2^+	0.729(7)						
3394.510(23)	**1697.117(28)**	1697.3	(4^+)	3^+	0.314(6)	0.275(15)	173^{+13}_{-12}	$+0.321^{+39}_{-47}$	0.53^{+18}_{-17}	0.0191^{+24}_{-21}	
								$+4.8^{+15}_{-9}$	5.47^{+62}_{-59}	0.00087^{+56}_{-40}	
	2190.185(25)	1204.3		2^+	0.601(7)			$(E2)$	3.05^{+27}_{-25}		

TABLE I. (*Continued.*)

E_{initial} (keV)	E_γ (keV)	E_{final} (keV)	J_i^π	J_f^π	B.R.	$\bar{F}(\tau)$	τ_{level} (fs)	δ or multipolarity	$B(E2)$ (W.u.)	$B(M1)$ (μ_N^2)	$B(E1)$ (mW.u.)
	2798.75(11)	595.9		2^+	0.085(5)			$(E2)$	0.127^{+17}_{-16}		
3408.739(59)	1944.788(51)	1463.9		4^+	1.000	0.225(45)	223^{+69}_{-47}				
3421.634(40)	**1957.709(39)**	1463.9		4^+	0.329(9)	0.687(26)	32(4)				
	2217.193(83)	1204.3		2^+	0.544(11)						
	2825.54(14)	595.9		2^+	0.127(7)						
3475.728(80)	**2879.757(71)**	595.9	$2, 3, 4^+$	2^+	1.000	0.277(36)	169^{+33}_{-26}				
3478.405(36)	1313.028(53)	2165.4	(6^+)	4^+	0.261(12)	0.040(23)	1500^{+2100}_{-600}	$(E2)$	2.0^{+13}_{-12}		
	2014.392(36)	1463.9		4^+	0.739(12)			$(E2)$	0.66^{+42}_{-39}		
3489.78(16)	**2893.80(14)**	595.9		2^+	1.000	0.022(40)	> 940				
3494.497(90)	**2898.487(94)**	595.9	2^+	2^+	0.907(8)	0.505(26)	66^{+7}_{-6}	$+5.5^{+36}_{-16}$	2.87(38)	0.0010^{+12}_{-7}	
								-0.215^{+73}_{-76}	0.13^{+13}_{-8}	0.0307(42)	
	3494.51(15)	0.0		0^+	0.093(8)			$E2$	0.120^{+23}_{-21}		
3500.824(60)	**2036.863(56)**	1463.9		4^+	0.751(16)	0.241(36)	202^{+45}_{-33}				
	2904.90(15)	595.9		2^+	0.249(16)						
3558.099(47)	2962.109(67)	595.9	1	2^+	0.455(18)	0.851(20)	13(2)				
	3558.016(54)	0.0		0^+	0.545(18)						
3566.628(46)	2361.93(12)	1204.3	$2, 3, 4^+$	2^+	0.132(10)	0.746(21)	24^{+3}_{-2}				
	2970.692(43)	595.9		2^+	0.868(10)						
3574.191(55)	**2369.859(73)**	1204.3		2^+	0.260(14)	0.890(27)	9.1^{+25}_{-24}				
	2978.181(65)	595.9		2^+	0.740(14)						
3579.408(90)	2115.43(10)	1463.9		4^+	0.488(29)	0.747(52)	24^{+7}_{-6}				
	2374.91(16)	1204.3		2^+	0.211(19)						
	2983.68(20)	595.9		2^+	0.301(22)						
3612.26(13)	**3016.28(12)**	595.9		2^+	1.000	0.224(68)	220^{+120}_{-70}				
3648.134(72)	3648.037(64)	0.0	1	0^+	1.000	0.611(29)	43(5)				
3674.57(14)	**3078.57(19)**	595.9	(2^+)	2^+	0.523(37)	0.420(64)	90^{+26}_{-20}	$(E2/M1)$	$\leqslant 0.93$	$\leqslant 0.011$	
	3674.48(17)	0.0		0^+	0.477(37)			$(E2)$	0.35^{+14}_{-10}		

[a]The γ ray energy is taken from level energy differences due to contamination from other origins.
[b]The branching ratio for the 1830 keV γ ray is quoted as an upper limit because it is an unresolved doublet. The branching ratios for the other γ rays from this level are then quoted as ranges; the lower limit for the values corresponds to using the upper limit for the 1830 keV γ ray, and the upper limit corresponds to using zero for the 1830 keV branch. The transition probabilities are quoted with similar ranges.

the present work are included. All spin assignments were experimentally determined from this work and were made based on the Legendre polynomial fits to the angular distributions and the resulting minima in χ^2 in comparison to CINDY [20] calculations as previously detailed.

An objective of this work was obtaining a comprehensive image of the low-lying states in ^{74}Ge. In pursuing this goal, we carefully examined and refuted a number of the levels placed in the Nuclear Data Sheets (NDS) [22] and the Evaluated Nuclear Structure Data File (ENSDF) [23].

A. Erroneous states: Previously reported levels not observed in the current study and refuted

An objective of this work was obtaining an inclusive image of the low-lying states in ^{74}Ge, which could be compared with theoretical calculations. If a comprehensive picture of the level structure is sought, it is important to confirm or reject levels placed in earlier work. As noted previously, in inelastic neutron scattering, the population of levels in the target nucleus is statistical and nonselective in nature, resulting in the excitation of all levels, both yrast and nonyrast states, with $J \leqslant 6$ and either positive or negative parity. In practice, we find that the most intense γ ray de-exciting a level will be observed using incident neutrons exceeding the threshold by 100 keV for low-spin states or 400 keV for higher-spin ($J = 5, 6$) states. These values account for both the cross section of the levels and the detection efficiency of the γ rays. Therefore, if the dominant γ-ray branch is not observed within this range of incident neutron energies, we refute the γ-ray placement; if none of the branches are observed, we also refute the existence of the level, labeling it an "erroneous state". In the most definitive cases, the γ ray(s) are not observed at any incident neutron energy, or they are observed with a threshold below or well above the purported level energy, indicating that the previous γ-ray placement is incorrect.

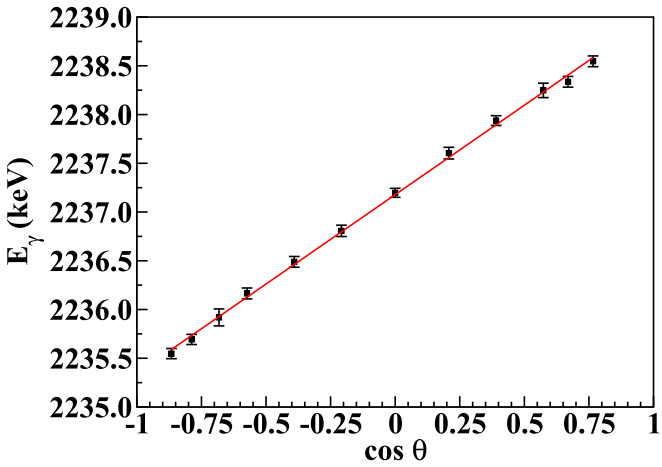

FIG. 3. Doppler-shift attenuation data for the 2237.1 keV γ ray from the 2833.0 keV 2^+ state. The lifetime was measured to be 28(1) fs.

Moreover, due to the wealth of data obtained from the $(n, n'\gamma)$ measurements, coincidence data are typically unnecessary to verify γ-ray placements. As already mentioned, the energies of the incident fast neutrons can be varied, thus the energy threshold of a γ ray is easily identified. Lifetime measurements provide additional evidence for γ-ray placements, as the lifetime determined for each decay branch must agree. Furthermore, γ-ray energies are usually determined sufficiently well that they can provide excellent evidence for placements in the level scheme. Finally, the spins of the levels can be identified by comparing both the level cross sections from the excitation functions with statistical model calculations, as well as with the angular distributions independently for each γ ray. Each branch must, of course, yield the same spin. All of these factors aid in the creation of a consistent picture of the level structure.

In pursuing our goal of a comprehensive level scheme, we carefully examined the placements of states in the NDS [22] and the ENSDF [23]. In the current study of ^{74}Ge, 11 previously placed states below 3 MeV were rejected, as the level placements were not supported by our data, as described above. These discrepancies are discussed in detail below, and we have eliminated these erroneous states from the level scheme. In cases where γ rays were reported in the decay of the proposed levels, we have searched for these decays without success. Levels falling in this category are:

(i) the 1724.954 keV (0^+) state purportedly observed with the (n, γ) reaction [16];
(ii) the 2878.14 keV level reported in a (p, p') reaction study [24] and in $(n, n'\gamma)$ reaction measurements with reactor neutrons [12]; and
(iii) the 2961.0 keV level identified in charged-particle [24,25] and neutron scattering studies [12].

Additional previously placed levels for which de-exciting γ rays had not been suggested (these occur primarily from charged-particle transfer reaction studies) and we found no γ decays in the current work included:

(i) a proposed 1913 keV 0^+ level reported only in transfer reactions studies [26,27];
(ii) a 2165 keV (1^-) level seen only in transfer reaction data [22];
(iii) a 2300 keV level with no spin assignment offered reported from the (^{6}Li, d) transfer reaction [28];
(iv) a 2490 keV level observed only in the (d, p) reaction [27];
(v) a 2572 keV 4^+ level reported in several charged-particle transfer and scattering reactions that may arise from a ^{70}Ge impurity [22,23];
(vi) a 2711 keV level observed only in a two-neutron transfer reaction [26]; and
(vii) a 2842 keV level reported only in (d, p) [26] and (α, α') [29] reaction studies.

Finally, we find no evidence for a 2403.5 keV spin-1 level reported from photon scattering measurements. A γ ray of approximately this energy is seen in our spectra, but with a neutron energy threshold of 3.1 MeV, indicating it originates from a level at 2999.2 keV as a transition to the first excited state, rather than to the ground state as previously reported [14]. More information is provided in the next section concerning the 2999.2 keV level, but Fig. 4 shows the threshold for both the 2403.2 keV γ ray and the ground-state branch. If the 2403.5 keV spin-1 state did exist, the cross section would be 30 mb at 2.6 MeV according to CINDY calculations; the expected ground-state transition would thus have approximately 10400 counts in the peak under our experimental conditions at 2.6 MeV in the excitation function measurement, but no peak is evident at all.

B. Newly reported levels and levels with new spectroscopic information

Most of the low-lying states in ^{74}Ge have been characterized in many reactions; however, some levels deserve special comments. Our starting point is the 2006 Nuclear Data Sheets evaluation by Singh and Farhan [22]. While transfer reaction data are frequently available for levels above 3 MeV, the uncertainties in the energies associated with these data make it difficult to assure that the state in question is the unique excited state. Therefore, with rare exceptions, above 3 MeV only γ-ray data are used in identifying levels and making spin-parity assignments. Also, we should remark that only seven levels (those at 595.9, 1204.3, 1697.3, 2226.5, 2973.7, 3104.8, and 3489.8 keV) of the 61 levels listed in Table I lack experimentally determined lifetimes in this work. For four of these levels, lifetime limits are established.

We note that, except for a state at 2690.7 keV, for which negative parity has been independently determined [15,30], we could assign spins and parities of all the states below 2860 keV with confidence from our data alone. We also believe that no states below 3 MeV have been omitted. Such a comprehensive picture is important as it now facilitates detailed comparisons with nuclear structure calculations and should lead to an improved understanding of the structure of this mass region.

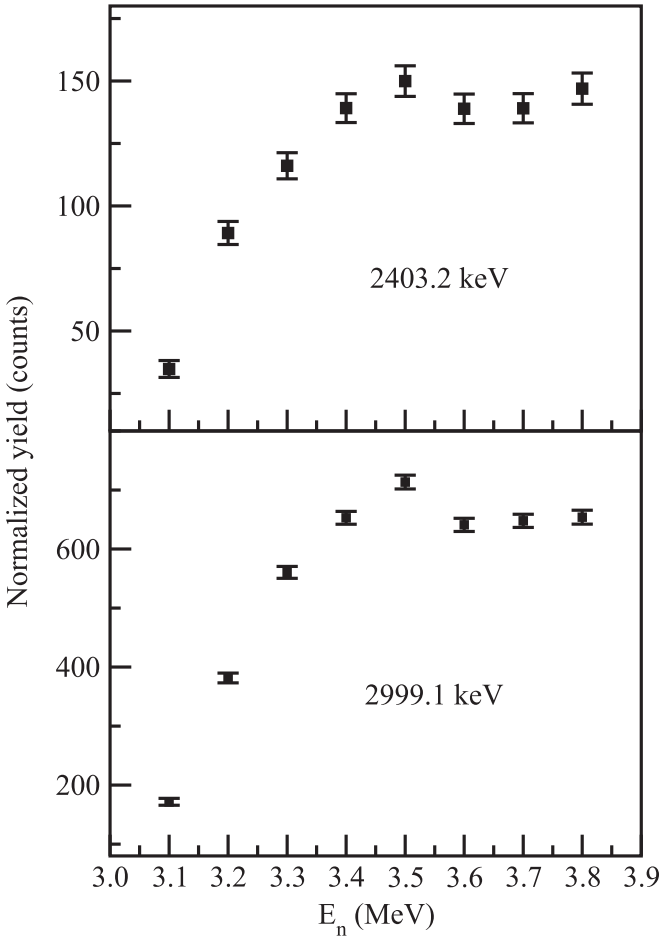

FIG. 4. Excitation functions for the 2403.2 and 2999.1 keV γ rays from the 2999.2 keV 2^+ state demonstrating the 3.1 MeV threshold and similar shapes for each.

1. Spin-1 states

As mentioned previously, new nuclear resonance fluorescence measurements have been completed using HIγS at TUNL in collaboration with Johnson *et al.* [18]. With the use of linearly polarized photons, spin-1 states are excited and the parities can be determined [31]. From the $(n, n'\gamma)$ reaction, we can readily determine the spin, but the parity is often more difficult. Therefore, for the spin-1 levels listed below, the parities from other reactions such as the recent NRF study [18] are discussed.

2690.7 keV 1 level: One new γ ray was assigned to this level, which has a spin of 1. While we cannot independently confirm the parity, a negative-parity assignment is available from (γ, γ') and $(\alpha, \alpha'\gamma)$ measurements [15,18,30].

3032.9 keV 1 level: Only a transition to the ground state is observed from this level with a spin of 1. However, (γ, γ') and $(\alpha, \alpha'\gamma)$ data collected by Negi *et al.* [15] and Johnson *et al.* [18] lead to a firm 1^- assignment.

3092.3 keV 1^+ level: This level, observed in the photon scattering measurements by Jung *et al.* [14], was given a $1^{(+)}$ assignment, and was also reported by Johnson *et al.* [18] and given firm positive parity. The observed mixing ratio for the transition to the second 2^+ state supports the assignment of positive parity. One new branch is also placed.

3275.7 keV 1 level: A spin-1 level at this energy was also identified in the (γ, γ') reaction [13,14], but the parity could not be determined. The level was not populated in the recent measurements due to experimental constraints [18]. The $(n, n'\gamma)$ reaction data agree with the spin, but do not allow a parity determination either. Two new decays are placed from the present work.

3558.1 keV 1 level: The present work is in agreement with a spin of 1. Originally assigned as 1^- by Jung *et al.* [14] in the (γ, γ') reaction, new measurements with polarized photons indicate that the parity is positive [18].

3648.1 keV 1 level: Originally assigned as 1^+ by Jung *et al.* [14] in the (γ, γ') reaction, more recent photon scattering [18] and $(\alpha, \alpha'\gamma)$ measurements [15] indicate negative parity.

2. Other states with new information

1463.9 keV 4^+ level: Although the uncertainties on the accepted lifetime of this level of $\tau = 2.21(15)$ ps [32] are smaller than those determined in the present experiment, 2.35^{+99}_{-54} ps, our measured lifetime is consistent with the previous determination. A more recent measurement [33] gives $\tau = 2.4$ ps, but without uncertainties.

2226.5 keV 0^+ level: The energy of this level differs by more than 1 keV from that given in the evaluation [22]. This discrepancy may be due to the existence of a triplet at ≈ 1630 keV, which we were able to resolve by varying the incident neutron energy. The other two members of the triplet originate from levels at 2.8 MeV, thus in the angular distribution at a neutron energy of 2.6 MeV, only the γ ray from the 2226.5 keV level is present in the spectra. Unfortunately, only a limit on the lifetime of this level could be obtained.

2536.6 keV 3^- level: The lifetime from our measurements agrees with the previous determination (350^{+200}_{-150} fs) [12] but displays considerably smaller uncertainties.

2600.3 keV 2^+ level: Three new branches were assigned to this state. The spin-parity assignment for this level now appears to be firm; however, the level lifetime reported here is not in agreement with the previous determination of 450^{+180}_{-140} fs [12].

2693.8 keV 3^- level: The limit on the level lifetime determined here is much different from that given in the data evaluation [22].

2697.1 keV 5^+ level: Although previously assigned as (2^+) [22], the 5^+ assignment is based on the angular distribution data and the population cross section compared with CINDY calculations. The decay branches appear to be firm.

2750.1 keV 0^+ level: The spin-parity of this state was established from (t, p) reaction measurements [26] and confirmed by the observation of de-exciting γ rays in $(n, n'\gamma)$ measurements [12]. Our excitation function and angular distribution measurements are both in agreement with this spin-parity assignment.

2828.7 keV 4^- level: The spin appears to be well established through (n, γ) measurements. This assignment is also supported by angular distributions of the current measurements. Negative parity is preferred, as the only branch, which

is to the 3_1^+ state, has a measured mixing ratio of 0 and thus is a pure $E1$ transition.

2833.0 keV 2^+ level: A new branch to the 2_2^+ state, which is part of the $\approx$ 1630 keV triplet is assigned. The lifetime, which is very well determined here (see Fig. 3), differs considerably from the previous measurement (13^{+6}_{-4} fs) [12]. The minimum in χ^2 for the dominate branch provides a spin of 2.

2836.2 keV 4^+ level: The spin-parity of this level was previously assigned as (2^+) [22], but our angular distribution data favor 4^+ in comparison with CINDY calculations. Two new γ rays were also assigned.

2857.3 keV 0^+ level: The spin-parity of this state was established from (p,t) [34,35] reaction measurements and the γ rays from this state were placed by Kosyak *et al.* [12]. Our data support this spin-parity assignment and the γ-ray placements.

2949.5 keV (2^-) level: This level which is strongly fed in β^- decay [36], likely has negative parity, but the spin could not be uniquely assigned from the available data. $J = 2$ is slightly preferred from the comparison of the angular distribution and excitation function with CINDY [20] calculations.

2973.7 keV 5^- level: This level, now assigned as $J^\pi = 5^-$, is observed in β^- decay [36], the (n,γ) reaction [16,37,38], and the $(^7\mathrm{Li}, 2np\gamma)$ reaction [11], and is observed to decay by two transitions to 4^+ states with negative a_2 coefficients and measured mixing ratios of zero, indicating pure $E1$ transitions. The excitation function cross section is also consistent with spin 5. In addition, the previously reported ground-state transition [22] is not observed.

2999.2 keV 2^+ level: Four decay branches, one new, are observed from this level, and the positive a_2 coefficient for the transition to the ground state leads to a unique 2^+ assignment. In addition, population of this state in the $(\alpha,\alpha'\gamma)$ measurements [15] supports the 2^+ assignment. Figure 4 demonstrates the excitation functions of the two strongest branches affirming their placement from this level.

3017.8 keV (2^+) level: This level was previously only reported from transfer data [22]; all γ rays are newly placed in the present work. $J^\pi = 2^+$ is favored from (t,p) and (p,t) reaction data in the NDS evaluation [22], and our γ-ray angular distribution data also favor this possibility based on the χ^2 minima in comparison with CINDY [20] calculations. No γ ray to the ground state is observed, however.

3034.1 keV 3^+ level: A $J = 3$ assignment is favored for this state, and most of the branches have measurable mixing ratios, indicating mixed $E2/M1$ transitions, and, therefore, positive parity. The 1829.9 keV γ ray is a doublet that cannot be resolved in our data, thus the branching ratios are quoted as ranges indicating upper and lower limits. The measured lifetime of the level differs considerably from the prior value (85^{+15}_{-10} fs) [12].

3081.7 keV 4^- level: While a (3^+) assignment is suggested in the evaluation [22], the angular distribution data favor $J = 4$ with values for the mixing ratio of the transition to the first 3^- state, indicating negative parity for this state. As such, the $E1$ transitions from this state lead to a 4^- assignment.

3104.8 keV 5^- level: This level has been observed in several reactions and is firmly assigned as 5^- in the data evaluation [22], with which the current data agree. Only one of the two γ rays reported previously is observed in the current work, however.

3175.5 keV 3^- level: While the data are consistent with the 3^- assignment; the measured lifetime is somewhat longer than that given from a previous determination (140^{+50}_{-40} fs) [12].

3199.3 keV 2^+ level: With four decay branches, three of which are new including a ground-state transition with a positive a_2 value, the 2^+ assignment [22] appears to be firm and is supported by observation of this state in $(\alpha,\alpha'\gamma)$ measurements [15]; however, the lifetime we measure is not consistent with the previous determination (34^{+11}_{-6} fs) [12].

3271.4 keV (4^-) level: Although a (2^+) assignment was suggested [22], (4^-) is favored from the angular distribution data. For the 1574 keV branch, the spin is definitively 4 as that is by far the solution with the lowest χ^2 value, the a_2 coefficient is negative and the mixing ratio is consistent with zero within uncertainties, indicating a pure $E1$ transition and thus negative parity.

3408.7 keV level: The level energy, as determined from the decay of a single γ ray, is much different from that observed in (n,γ) measurements [39], thus raising the question as to whether this is the state observed previously.

3494.5 keV 2^+ level: This level has not been reported in prior measurements. The spin assignment is based primarily on the observed positive a_2 coefficient for the angular distribution of the transition to the ground state and the measurable $E2/M1$ mixing ratio of the transition to the first excited state.

3500.8 keV level: This level may correspond to the level observed at 3501.4 keV previously [22].

3566.6 keV $(2,3,4^+)$ level: This level decays to the first two excited 2^+ states and exhibits a short lifetime; however, the spin-parity could not be assessed from the available data.

3579.4 keV level: Although the spin was assigned as 2^+ in the evaluation [22], this could not be confirmed from the current data. Two new branches are placed, however.

Levels from this work but not reported previously include: 2875.0 keV (3^+); 3180.1 keV $(2,3,4^+)$; 3219.9 keV (5^+); 3336.8 keV $4,5^+,6^+$; 3359.2 keV; 3386.5 keV $2,3,4^+$; 3394.5 keV (4^+); 3421.6 keV; 3475.7 keV $2,3,4^+$; 3489.8 keV; 3494.5 keV 2^+; 3500.8 keV; 3574.2 keV; 3612.3 keV; 3674.6 keV (2^+).

IV. SHELL-MODEL CALCULATIONS

As in our recent studies of ^{76}Ge [8] and ^{76}Se [9], configuration interaction (CI) shell-model calculations in the $jj44$ model space, consisting of the $0f_{7/2}, 1p_{3/2}, 1p_{1/2}, 0g_{9/2}$ orbitals for protons and neutrons, were performed with the code NuShellX [40]. We utilize two common Hamiltonians derived for the $jj44$ model space: $JUN45$ [41] and $jj44b$ [8]. These are both data-driven Hamiltonians obtained from a single-valued decomposition (SVD) fit to binding energy and excitation energy data as described in the Appendix of Ref. [8]. The main difference between the $JUN45$ and $jj44b$ Hamiltonians is the regions of data that were used for the SVD fit [8].

A comparison of the calculated levels obtained using the $JUN45$ Hamiltonian with experimental data up to 3 MeV

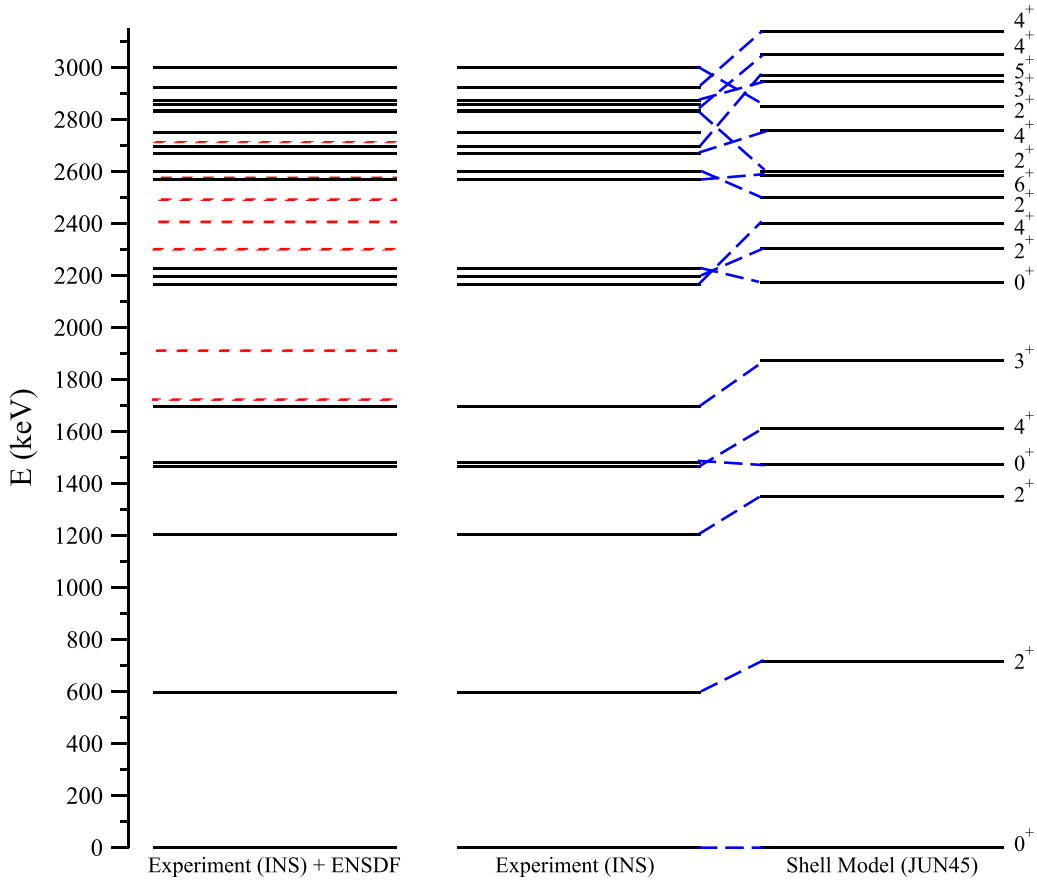

FIG. 5. Comparison of experimental positive-parity levels with shell-model calculations. The left panel shows all reported positive-parity levels including those refuted in the current work. The middle panel shows just those confirmed in the present experiments, and the right panel shows the calculated levels and agreement with the current results.

is shown in Fig. 5. The erroneous levels from ENSDF [23] cannot be accounted for by the calculations. The calculations were performed independently and had no input from the current experimental results. (The only ^{74}Ge data used for the SVD fit in Ref. [41] were the ground-state binding energy and the excitation energies of the lowest two 2^+ states.)

Calculated $B(E2)$ values for transitions between low-lying states are shown in Fig. 6, which also gives experimental values when they are available. We used the same $E2$ effective charges of $e_p = 1.8$ and $e_n = 0.8$ that were used in Refs. [8] and [9]. The overall agreement between experiment and theory is rewarding and is even more impressive than our comparisons for ^{76}Ge [8]. A similar level of agreement with experimental $B(E2)$ values is obtained with the $jj44b$ [9] Hamiltonian.

The energy level comparison up to 4 MeV with both the $JUN45$ and $jj44b$ Hamiltonians is shown in Fig. 7. The horizontal lines in the figure are proportional to the J value, with those in red for positive-parity states, and those in blue for negative-parity states. Some of the J^π values are labeled as a guide. For the experimental data depicted on the left-hand side, the levels with an uncertain J^π are shown by black dots. There are a total of 109 experimental levels up to 4 MeV, compared with 76 levels for $JUN45$ and 85 levels for $jj44b$. As we have found for states below 3 MeV, some of the experimental levels given in NDS [22] and the ENSDF [23] between 3 and 4 MeV may be spurious. The negative-parity levels for $jj44b$ start at 2.5 MeV in agreement with experiment. The negative-parity levels for $JUN45$ start at 3.2 MeV.

For the region from 4 to 11 MeV, we use the extrapolated Lanczos matrix (ELM) method of Ref. [42]. The results for the cumulative number of levels up to 11 MeV are shown in Fig. 8. The level densities for positive- and negative-parity states up to 5 MeV are rather different, but above 5 MeV, the level density does not depend on parity. The total number of levels up to 10.20 MeV is about 29,000 for $jj44b$ and 45,000 for $JUN45$. We conclude the level density calculated in the $jj44$ model space has an uncertainty of about a factor of 2. Above 5 MeV, the calculated level density is in good agreement with experiment [43] shown by the green points in Fig. 8. The error band for the experimental points is shown in Fig. 11 of Ref. [43]. Around 3 MeV the experimental level-density data from [43] is too high largely because it includes erroneous levels in the NDS [22] below 4 MeV that were used in [43]. It is likely that the level density for these intruder states around 10 MeV will be important for the total. One may speculate that the total level density has close to an exponential behavior above about 6 MeV (e.g., linear in E_x on the $\log_{10}$ plot).

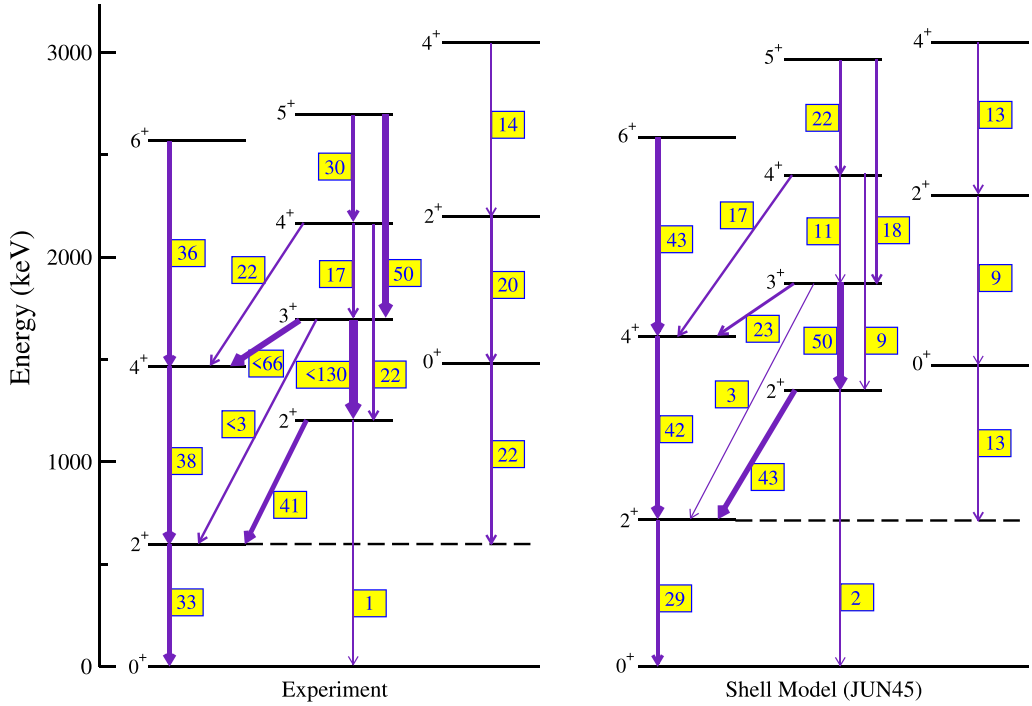

FIG. 6. Comparison of positive-parity states and transitions of interest in the ^{74}Ge level scheme with shell-model calculations using the *JUN*45 interaction. $B(E2)$ values in W.u. are shown on the transition arrows highlighted in yellow. The left portion is the ground-state band, the center the γ band, and the right the shape-coexisting band.

V. DISCUSSION

The stable Ge nuclei have been described as a region of rapid nuclear shape evolution and shape coexistence [1,2], and Ayangeakaa *et al.* [3,5,6] have demonstrated that triaxially deformed configurations play a significant role in the low-lying structure. Moreover, ^{74}Ge has been suggested as the nucleus representing the transition from soft to rigid triaxiality [11]. The fusion-evaporation study of ^{74}Ge with the ^{70}Zn(^{7}Li, $2np$) reaction by Sun *et al.* [11] contributed an extensive band structure in ^{74}Ge, and they concluded from the energy staggering pattern in the γ band (Band 3 in Ref. [11]) that the triaxiality of ^{74}Ge evolves from γ soft (similar to ^{72}Ge) at low spin [3] to γ rigid (similar to ^{76}Ge) at higher spin [5].

In comparing the experimentally observed energy levels and their properties with model calculations, it is useful to

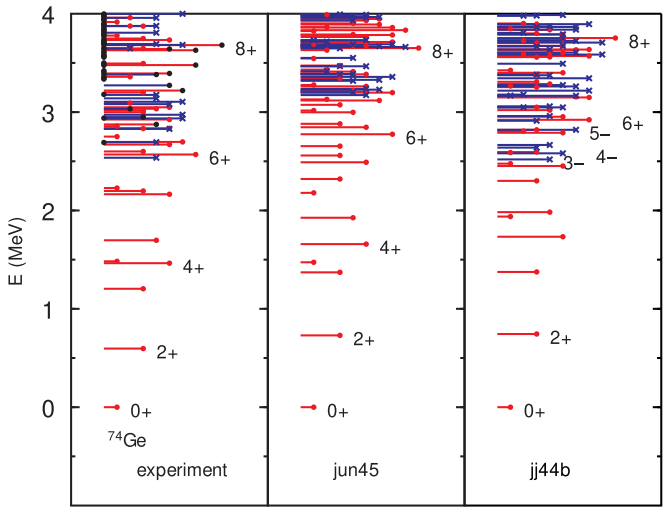

FIG. 7. Experimental levels up to 4 MeV compared to full Lanczos-based calculations. The horizontal lines in the figure are proportional to the J value with those in red for positive-parity states, and those in blue for negative-parity states. Some of the J^{π} values are labeled as a guide. For the experimental data shown on the left-hand side, the levels with an uncertain J^{π} are shown by black dots.

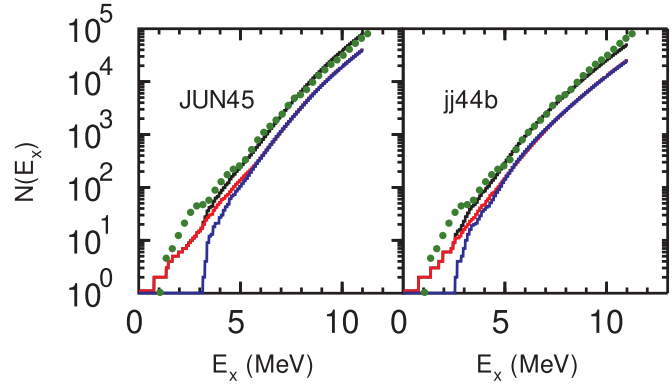

FIG. 8. Results for the cumulative number of levels up to 11 MeV based on the ELM method. The red lines are the results for positive-parity states and the blue lines are the results for negative parity states. The black lines are the total for both parities. The greens points are the experimental data from [43].

affirm that we have identified all the excited states up to some energy, i.e., about 2.8 MeV in the case of ^{74}Ge. Similar comparisons are not possible for most other nuclei in the region; their level structures are not known in sufficient detail. With this evaluated set of levels, meaningful comparisons with theoretical calculations can be pursued, with the expectation that a one-to-one correspondence of calculated and experimental states would be obtained. This comparison is shown in Fig. 5, where no adjustment of the parameters used in the shell-model calculation was attempted. A one-to-one correlation of experimental and theoretical levels was found up to 2.8 MeV. Given this success, all levels up to 10.2 MeV where then calculated. This effort allowed a study of the level density, which indicates that the total level density has near exponential character. The agreement with the experimental data above 4 MeV in excitation from Ref. [43] is excellent.

Several collective features in ^{74}Ge emerge from this study. In addition to the ground band and the aforementioned γ band, the 2^+ mixed-symmetry state is identified at 2833 keV with $B(M1; 2^+_{ms} \rightarrow 2^+_1) = 0.176\,\mu_N^2$, where the shell-model prediction is for a state at 2601 keV and $B(M1; 2^+_{ms} \rightarrow 2^+_1) = 0.256\,\mu_N^2$. A similar excitation was observed at 2767 keV in ^{76}Ge [8]. Also, the well-developed 0^+, 2^+, 4^+ shape-coexisting structure, which is reproduced very well by the shell-model calculations, is evident. Note, however, that it is the fourth calculated 4^+ state yet the sixth experimental one, which decays to the 2^+ state of the shape-coexisting band with a significant $B(E2)$ value which is shown in Fig. 6.

The low-lying 0^+ excitations in the stable Ge isotopes are described in detail in the review by Heyde and Wood [1], which points to the role of subshells and pairing in understanding shape coexistence. Most of the experimental and theoretical studies of shape coexistence in this region have focused on elucidating the wave functions of the ground states and the first excited 0^+ states of the Ge nuclei; a detailed picture of these states and the configurations giving rise to these states has emerged [1]. On the other hand, it appears that the bands built on these 0^+ excitations have not been well characterized previously. Although bands have been established to spin 10^+ in ^{68}Ge, to 8^+ in ^{70}Ge, and to 6^+ in ^{72}Ge [23], few level lifetimes are available, and the large $B(E2)$s demonstrating the expected collectivity have not been identified, i.e., the collectivity of these band structures is simply not well established. In the present work, the 2^+ and 4^+ states built on the 1483 keV 0^+ state were observed at 2198 and 3049 keV, respectively, and the collectivity of these states is supported by the measured $B(E2)$ values. This band thus represents the best example of shape coexistence in the Ge nuclei to date.

VI. CONCLUSION

Low-lying levels in ^{74}Ge were investigated with the $(n, n'\gamma)$ reaction, and a revised level scheme is presented. Basic structures—including the ground band, γ band, shape-coexisting band, and the mixed-symmetry 2^+ state—have been observed. The $B(E2)$s reported here permit meaningful comparisons with large-scale shell-model calculations. Remarkably, the shell-model calculations yield excellent agreement with each of these structural features. The number of levels up to 2.8 MeV was reproduced as well, which motivated calculations of the level density. The $JUN45$ Hamiltonian has been used in the $jj44$ model space to obtain nuclear matrix elements (NME) for neutrinoless double-β decay [10]. The agreement with the level energy data for ^{74}Ge provides confidence in the valence-space structure used for these NME calculations.

ACKNOWLEDGMENTS

We wish to thank H. E. Baber for his many contributions to these measurements. We also gratefully acknowledge W. B. Walters for providing data prior to publication and for making us aware of unpublished data, D. Negi for providing information beyond their published work, and S. R. Johnson and R. V. F. Janssens for sharing their photon scattering results even prior to publication. This material is based upon work supported by the U.S. National Science Foundation under Grants No. PHY-1913028, No. PHY-2209178, and No. PHY-2110365.

[1] K. Heyde and J. L. Wood, Rev. Mod. Phys. **83**, 1467 (2011).
[2] P. E. Garrett, M. Zielińka, and E. Clément, Prog. Part. Nucl. Phys. **124**, 103931 (2022).
[3] A. D. Ayangeakaa, R. V. F. Janssens, C. Y. Wu, J. M. Allmond, J. L. Wood, S. Zhu, M. Albers, S. Almaraz-Calderon, B. Bucher, M. P. Carpenter, C. J. Chiara, D. Cline, H. L. Crawford, H. M. David, J. Harker, A. B. Hayes, C. R. Hoffman, B. P. Kay, K. Kolos, A. Korichi, T. Lauritsen, A. O. Macchiavelli, A. Richard, D.Seweryniak, and A. Wiens, Phys. Lett. B **754**, 254 (2016).
[4] Y. Toh, C. J. Chiara, E. A. McCutchan, W. B. Walters, R. V. F. Janssens, M. P. Carpenter, S. Zhu, R. Broda, B. Fornal, B. P. Kay, F. G. Kondev, W. Królas, T. Lauritsen, C. J. Lister, T. Pawłat, D. Seweryniak, I. Stefanescu, N. J. Stone, J. Wrzesiński, K. Higashiyama, and N. Yoshinaga, Phys. Rev. C **87**, 041304(R) (2013).
[5] A. D. Ayangeakaa, R. V. F. Janssens, S. Zhu, D. Little, J. Henderson, C. Y. Wu, D. J. Hartley, M. Albers, K. Auranen, B. Bucher, M. P. Carpenter, P. Chowdhury, D. Cline, H. L. Crawford, P. Fallon, A. M. Forney, A. Gade, A. B. Hayes, F. G. Kondev, Krishichayan, T. Lauritsen, J. Li, A. O. Macchiavelli, D. Rhodes, D. Seweryniak, S. M. Stolze, W. B. Walters, and J. Wu, Phys. Rev. Lett. **123**, 102501 (2019).
[6] A. D. Ayangeakaa, R. V. F. Janssens, S. Zhu, J. M. Allmond, B. A. Brown, C. Y. Wu, M. Albers, K. Auranen, B. Bucher, M. P. Carpenter, P. Chowdhury, D. Cline, H. L. Crawford, P. Fallon, A. M. Forney, A. Gade, D. J. Hartley, A. B. Hayes, J. Henderson, F. G. Kondev, Krishichayan, T. Lauritsen, J. Li, D. Little, A. O. Macchiavelli, D. Rhodes, D. Seweryniak, S. M. Stolze, W. B.Walters, and J. Wu, Phys. Rev. C **107**, 044314 (2023).

[7] M. Agostini, G. Benato, J. A. Detwiler, J. Menéndez, and F. Vissani, Rev. Mod. Phys. **95**, 025002 (2023).
[8] S. Mukhopadhyay, B. P. Crider, B. A. Brown, S. F. Ashley, A. Chakraborty, A. Kumar, M. T. McEllistrem, E. E. Peters, F. M. Prados-Estévez, and S. W. Yates, Phys. Rev. C **95**, 014327 (2017).
[9] S. Mukhopadhyay, B. P. Crider, B. A. Brown, A. Chakraborty, A. Kumar, M. T. McEllistrem, E. E. Peters, F. M. Prados-Estévez, and S. W. Yates, Phys. Rev. C **99**, 014313 (2019).
[10] B. A. Brown, M. Horoi, and R. A. Sen'kov, Phys. Rev. Lett. **113**, 262501 (2014).
[11] J. J. Sun, Z. Shi, X. Q. Li, H. Hua, C. Xu, Q. B. Chen, S. Q. Zhang, C. Y. Song, J. Meng, X. G. Wu, S. P. Hu, H. Q. Zhang, W. Y. Liang, F. R. Xu, Z. H. Li, G. S. Li, C. Y. He, Y. Zheng, Y. L. Ye, D. X. Jiang *et al.*, Phys. Lett. B **734**, 308 (2014).
[12] Y. G. Kosyak, L. V. Chekushina, and A. S. Ermatov, Bull. Russ. Acad. Sci. Phys. **67**, 151 (2003).
[13] R. Massarczyk, R. Schwengner, L. A. Bernstein, M. Anders, D. Bemmerer, R. Beyer, Z. Elekes, R. Hannaske, A. R. Junghans, T. Kögler, M. Röder, K. Schmidt, A. Wagner, and L. Wagner, Phys. Rev. C **92**, 044309 (2015).
[14] A. Jung, S. Lindenstruth, H. Schacht, B. Starck, R. Stock, C. Wesselborg, R. D. Heil, U. Kneissl, J. Margraf, H. H. Pitz, and F. Steiper, Nucl. Phys. A **584**, 103 (1995).
[15] D. Negi, M. Wiedeking, E. G. Lanza, E. Litvinova, A. Vitturi, R. A. Bark, L. A. Bernstein, D. L. Bleuel, S. Bvumbi, T. D. Bucher, B. H. Daub, T. S. Dinoko, J. L. Easton, A. Görgen, M. Guttormsen, P. Jones, B. V. Kheswa, N. A. Khumalo, A. C. Larsen, E. A. Lawrie *et al.*, Phys. Rev. C **94**, 024332 (2016).
[16] C. Hofmeyr, C. Franklyn, G. Barreau, H. Börner, R. Brissot, H. Faust, and K. Schreckenbach, Nuclear Data Sheets (private communication).
[17] W. B. Walters (private communication).
[18] S. R. Johnson, R. V. F. Janssens, U. Friman-Gayer, B. A. Brown, B. P. Crider, S. W. Finch, Krishichayan, D. R. Little, S. Mukhopadhyay, E. E. Peters, A. P. D. Ramirez, J. A. Silano, A. P. Tonchev, W. Tornow, and S. W. Yates, Phys. Rev. C **108**, 024315 (2023).
[19] T. Belgya, G. Molnár, and S. W. Yates, Nucl. Phys. A **607**, 43 (1996).
[20] E. Sheldon and V. C. Rogers, Comput. Phys. Commun. **6**, 99 (1973).
[21] K. Krane, R. Steffen, and R. Wheeler, At. Data Nucl. Data Tables **11**, 351 (1973).
[22] B. Singh and A. R. Farhan, Nucl. Data Sheets **107**, 1923 (2006).
[23] ENSDF database, www.nndc.bnl.gov/ensdf (2023).
[24] R. Tamisier, B. Ramstein, P. Avignon, L. H. Rosier, G. La Rana, F. Guilbault, C. Lebrun, and C. Jeanperrin, Nucl. Phys. A **385**, 430 (1982).
[25] G. Szaloky, L. A. Montestruque, M. C. Cobian-Rozak, and S. E. Darden, Phys. Rev. C **18**, 750 (1978).
[26] S. Lafrance, S. Mordechai, H. T. Fortune, and R. Middleton, Nucl. Phys. A **307**, 52 (1978).
[27] M. Dojo, Nuclear Data Sheets (private communication).
[28] D. Ardouin, D. L. Hanson, and N. Stein, Phys. Rev. C **22**, 2253(R) (1980).
[29] B. Schürmann, D. Rychel, B. van Krüchten, J. Speer, and C. A. Wiedner, Nucl. Phys. A **475**, 361 (1987).
[30] D. Negi (private communication).
[31] A. Zilges, D. Balabanski, J. Isaak, and N. Pietralla, Prog. Part. Nucl. Phys. **122**, 103903 (2022).
[32] Y. Toh, T. Czosnyka, M. Oshima, T. Hayakawa, H. Kusakari, M. Sugawara, Y. Hatsukawa, J. Katakura, N. Shinohara, and M. Matsuda, Eur. Phys. J. A **9**, 353 (2000).
[33] G. Gürdal, E. A. Stefanova, P. Boutachkov, D. A. Torres, G. J. Kumbartzki, N. Benczer-Koller, Y. Y. Sharon, L. Zamick, S. J. Q. Robinson, T. Ahn, V. Anagnostatou, C. Bernards, M. Elvers, A. Heinz, G. Ilie, D. Radeck, D. Savran, V. Werner, and E. Williams, Phys. Rev. C **88**, 014301 (2013).
[34] F. Guilbault, D. Ardouin, J. Uzureau, P. Avignon, R. Tamisier, G. Rotbard, M. Vergnes, Y. Deschamps, G. Berrier, and R. Seltz, Phys. Rev. C **16**, 1840 (1977).
[35] A. C. Rester, J. B. Ball, and R. L. Auble, Nucl. Phys. A **346**, 371 (1980).
[36] H. W. Taylor, R. L. Schulte, P. J. Tivin, and H. Ing, Can. J. Phys. **53**, 107 (1975).
[37] M. A. Islam, T. J. Kennett, and W. V. Prestwich, Phys. Rev. C **43**, 1086 (1991).
[38] J. Honzátko, I. Tomandl, A. M. Sukhovoi, and V. A. Khitrov, Bull. Russ. Acad. Sci. Phys. **68**, 1324 (2004).
[39] R. E. Chrien, D. I. Garber, J. L. Holm, and K. Rimawi, Phys. Rev. C **9**, 1839 (1974).
[40] B. A. Brown and W. D. M. Rae, Nucl. Data Sheets **120**, 115 (2014).
[41] M. Honma, T. Otsuka, T. Mizusaki, and M. Hjorth-Jensen, Phys. Rev. C **80**, 064323 (2009).
[42] W. E. Ormand and B. A. Brown, Phys. Rev. C **102**, 014315 (2020).
[43] A. V. Voinov, T. Renstrøm, D. L. Bleuel, S. M. Grimes, M. Guttormsen, A. C. Larsen, S. N. Liddick, G. Perdikakis, A. Spyrou, S. Akhtar, N. Alanazi, K. Brandenburg, C. R. Brune, T. W. Danley, S. Dhakal, P. Gastis, R. Giri, T. N. Massey, Z. Meisel, S. Nikas, S. N. Paneru, C. E. Parker, and A. L. Richard, Phys. Rev. C **99**, 054609 (2019).